Nanotechnology Perceptions
ISSN 1660-6795
www.nano-ntp.com

Evaluation Of Antimicrobial, Antioxidant, And Toxicological Assay (Zebrafish Model) Of Selenium Nanoparticles From Cinnamomum Verum

Archana Behera[1], Gautham Paul[1], Vinushya Selvam[2], Iadalin Ryntathiang[1], Mukesh Kumar Dharmalingam Jothinathan*[1]

[1.] *Centre for Global Health Research, Saveetha Medical College and Hospitals, Saveetha Institute of Medical and Technical Sciences (SIMATS), Saveetha University, Chennai, Tamil Nadu, India.*
[2.] *Department of Paediatrics, Saveetha Medical College and Hospitals, Saveetha Institute of Medical and Technical Sciences (SIMATS), Saveetha University, Chennai, Tamil Nadu, India.*
[1]**Corresponding author Email id: itsmemukesh@gmail.com (Mukesh Kumar Dharmalingam Jothinathan)*
Authors Mail ID:
[1]*Archana Behera: archanabc1998@gmail.com*
[1]*Gautham Paul: gauthampaul123@gmail.com*
[2]*Vinushya Selvam: selvamvinushya@gmail.com*
[1]*Iadalin Ryntathiang: iadalin.rynth.syiem@gmail.com*

Advances in nanotechnology have enabled the creation of a nanoparticulate form of selenium (Se) that exhibits versatility in its applications across various functional domains. Se is a crucial micronutrient that plays a critical role in the survival of all mammals and participates in the optimal functioning of human physiological functions. The available empirical evidence indicates that Selenium Nanoparticles (SeNPs) possess significant antioxidant and antimicrobial properties. This paper presents the production of SeNPs using Cinnamomum verum extract, with a focus on their antimicrobial, antioxidant, and toxicological properties. The antioxidant effectiveness of SeNPs was evaluated using 2,2-diphenyl-1-picrylhydrazyl (DPPH), hydrogen peroxide (H_2O_2), Ferric Reducing Antioxidant Power (FRAP), nitric oxide, and 2,2′-azinobis (3-ethylbenzthiazolin-6-sulfonic acid) (ABTS) assays. The results demonstrate that SeNPs exhibit significant ascorbic acid-based free radical scavenging activity. The effectiveness of SeNPs against prevalent pathogens was evaluated. The SeNPs demonstrated significant microbial efficacy using, time-kill curve analysis and protein leakage analysis methods, which exhibit concentration-dependent suppression of microbial proliferation, rendering them highly promising as antimicrobial therapeutics. Furthermore, the toxicological impacts of SeNPs were examined in zebrafish embryos as a model organism. Variations in SeNPs levels were administered, and their effects on embryonic development were monitored longitudinally. The findings of this study demonstrated a response to

dosage, whereby higher concentrations resulted in elevated mortality rates and developmental defects in zebrafish embryos. The toxicological assessment highlights the importance of precise dosage calculation in the context of potential biomedical applications, despite their benefits. This study emphasized the potential of SeNPs as eco-friendly antioxidants and antimicrobial agents. However, this underscores the need for further investigation into their safety profile, particularly in the context of biological applications.

Keywords: Cinnamomum verum, Selenium nanoparticles, Antioxidant activity, antimicrobial activity, zebrafish embryos, toxicology study,

1. Introduction

Numerous industries, including food, agriculture, electronics, medicine, drug delivery, therapies, and diagnostics, are seeing a significant rise in the use of nanotechnology. Nanoparticles can as vehicles for adjuvants, vaccinations, and antibiotics [Ghaderi et al., 2022]. The fast biosynthesis of metal nanoparticles, including gold, silver, selenium, MgO, CuO, and ZnO, has been successfully investigated in plants. Because medications attached to nanoparticles can deeply enter organs, the use of nanoparticles in cancer drug delivery is widespread. In particular, selenium, an important dietary vitamin present in Selenium Nanoparticles (SeNPs), is a novel therapeutic nanocarrier in medicine because of SeNPs' potent antibacterial and antioxidative properties [Alagesan et al., 2019].

Se is essential for thyroid metabolism, human fertility, enzyme activation, cellular metabolism, bodily defense against free radicals, and several other energy-related processes. The biological applications of selenium have been successful in various fields, such as molecular biology, biochemistry, genetics, and health. These fields include the use of selenium in immunomodulatory, antioxidant, antitumor, enzyme inhibitor, and anti-infective formulations [Alghuthaymi et al., 2021]. The Lauraceae family includes the evergreen Cinnamomum verum tree, which is widely distributed throughout Sri Lanka and other Asian nations. Indian traditional medicine treats bacterial, fungal, and inflammatory conditions using various plant parts. Several biological activities, including antibacterial, antibiofilm, anthelmintic, anticancer, and antifungal properties, have been found in cinnamon bark extract, making it one of the main bioactive substances Because of all of its biological potential [Ansari et al., 2020].

In the current investigation, C. verum bark extract was used for the green synthesis of ZnONPs and, AgNPs because of its extensive biological potential [Gulcin et al., 2019]. An essential oil, including eugenol and cinnamaldehyde, is extracted from the bark. Cinnamaldehyde has been linked to several biological actions, including cytotoxic, antimutagenic, anticancer, antifungal, and peripheral vasodilatory effects [Abu-Elghait et al., 2021]. SeNPs were characterized using several instrumental analytical techniques. Color shifts in the solution were utilized to visually monitor SeNPs formation during the incubation stage using UV/Vis Spectroscopy, Fourier Transform Infrared Spectroscopy (FTIR), and Scanning Electron Microscopy (SEM) with Energy-Dispersive X-ray Spectroscopy (EDAX) [Yilmaz et al., 2021, Salem et al., 2022, Munteanu et al., 2021]. The synthesized SeNPs were tested for their antioxidant capabilities by scavenging 2,2-diphenyl-1-picrylhydrazyl (DPPH) and hydroxyl (OH) radicals. The Ferric Reducing Antioxidant Power (FRAP) test is a widely used technique based on the Selective

Electron Transfer (SET) method. The results evaluate the ability of antioxidants under acidic conditions to reduce the ferric ions (Fe3+)-ligand complex, resulting in the formation of the luminescent ferrous complex (Fe2+). The 2,2′-azinobis (3-ethylbenzthiazolin-6-sulfonic acid) (ABTS) test evaluates the capacity of antioxidants to counteract the blue-green chromophore of maximum absorption, ABTS stable radical cation, which decreases in color intensity when antioxidants are present. [Gulcin et al., 2020, Bi et al., 2024]. Experiments with antioxidants demonstrated that the phytochemicals contained in SeNPs contribute to electrons and hydrogen. Therefore, by converting free radicals into more stable compounds, they should be able to terminate free radical chain reactions with an oxygen–oxygen single bond; hydrogen peroxide (H_2O_2) is the most basic peroxide. It is fragile and breaks down gradually upon exposure to light. All biological systems, including the human body, contain H_2O_2. Enzymes that use or break down H_2O_2 are categorized as peroxidases [Hariharan et al., 2024].

Cell lines and simple organisms are valuable tools for studying cell-level toxicity and genotoxicity. However, to obtain a comprehensive understanding of complex physiological interactions, it is imperative to use higher vertebrates. However, because of their large size, rodent models require substantial amounts of material for testing, have relatively slow and inaccessible embryo development, are expensive, and raise ethical questions about their use. In contrast, primate models have similar problems, but to a much greater extent. Zebrafish embryos are more advantageous for toxicity investigations due to their optical transparency, physiological responsiveness to xenobiotics, and resemblance to human tissue types and genome. Zebrafish embryos were treated with different amounts of SeNPs for toxicity experiments [Chandramohan et al., 2019, Haque et al., 2018].

2. Materials and methods:

SeNPs were synthesized using C. verum bark extract and characterized using various assays. C. verum bark was collected from Chennai, Tamilnadu, India. The Center for Advanced Studies in Botany reviewed the samples at the University of Madras, Chennai, India. The preparation of C. verum bark powder and its aqueous extraction procedure were performed as described in a previous study [Behera et al., 2024a]. Figure 1 displays a graphical abstract of the green synthesis of SeNPs using plant extracts.

2.1 Synthesis and characterization of Selenium nanoparticles

A 5 mM sodium selenite (Na_2SeO_3) solution was prepared by dissolving it in 200 mL of distilled water. To synthesize SeNPs, 50 mL of C. verum bark extract was mixed with 150 mL of a Na_2SeO_3 solution. The acidity level of reaction mixture was consistently checked and recorded. Subsequently, the reaction mixtures were incubated in a dark room on a rotating shaker at 40°C and 300 rpm for 3 h. Visual evaluation of the reaction mixture's color was followed by incubation at room temperature for 72 h. After the incubation period, a total color change was detected in the reaction mixture, indicating the successful synthesis of the nanoparticles. Conversely, the control containing only $SeCl_2$ exhibited no color change.

The SeNPs were characterized using UV- vis spectroscopy, FTIR spectroscopy, and SEM with EDAX. Synthesis was first detected using UV-visible spectrophotometry in the 200-800 nm range. The FTIR analysis, at 4000-400 cm^{-1}, successfully identified the specific functional groups present on the SeNPs. Morphology and purity were evaluated using SEM and EDAX. Figure 2 shows a graphical abstract of the application of the synthesized SeNPs [Behera et al., 2024a].

2.2 Antioxidant activity:

2.2.1 DPPH radical scavenging assay:

Each experiment involved the dilution of a 0.1 mM DPPH stock solution in methanol to a final concentration of 20 µM. SeNPs (10-50 µg/mL) were introduced into 200 µL of the DPPH solution and incubated in the dark for 10 min at ambient temperature. The absorbance was measured using methanol as, the blank. The DPPH scavenging activity was determined using a previously reported methodology [Wu et al., 2020].

2.2.2 Hydrogen peroxide radical scavenging assay

The H_2O_2 scavenging activity of SeNPs generated by biosynthesis was assessed using a 40 mM H_2O_2 solution in phosphate buffer at pH of 7.4. SeNPs and ascorbic acid (10-50 µg/mL) were added to 0.6 mL of the H_2O_2 solution and incubated for 10 min. Absorbance was determined using Vitamin C as the reference standard. The calculation of H_2O_2 scavenging activity was calculated following previous research [Rajakumari et al., 2020].

2.2.3 FRAP ASSAY:

A solution containing 2.3 mL of FRAP reagent was combined with 0.7 mL of SeNPs at different concentrations ranging from 10 to 50 µg/mL. The solution was subsequently incubated at 37ºC for 30 min. A spectrophotometer was used to measure the absorbance in a blank solution containing all chemicals. An increase in the absorbance of the reaction mixture indicates an enhanced reduction capability. The samples were acquired in triplicate. Ascorbic acid was used as the reference standard [Rajakumari et al., 2020].

2.2.4 ABTS:

The radical scavenging of ABTS was assessed following a prior investigation [Rajakumari et al., 2020]. 250 µL of ABTS+ and 20 µL of sample (10-50 µg/mL) were combined in a 96-well plate. The standard reference in this study was ascorbic acid, and ethanol was used as the blank. The absorbance was assessed.

2.2.5 Nitric Oxide Assay:

The nitric oxide radical inhibition assay was examined using previous experiments [Vinothkanna et al., 2023]. Incubation was performed on a reaction mixture (3 mL) containing

sodium nitroprusside (10 mm, 2 mL), phosphate buffer saline (0.5 mL), and either SeNPs (10-50 µg/mL) or a reference solution (ascorbic acid, 0.5 mL). Following the incubation period, a volume of 0.5 mL from the reaction mixture was combined with 1 mL of sulfanilic acid reagent (0.33 % in 20% glacial acetic acid) and left undisturbed for 5 min to ensure thorough diazotization. Subsequently, 1 mL of naphthyl ethylene diamine dihydrochloride was introduced, thoroughly blended, and left undisturbed for 30 min at 25°C. When exposed to diffused light, a pink chromophore is generated. The absorbance of these solutions were quantified at a wavelength of 540 nm compared with the equivalent blank solutions.

2.3 Antimicrobial Activity

Antimicrobial activity was evaluated using SeNPs synthesized from C. verum extract using the agar well diffusion method. Bacterial were selected as Enterococcus faecalis, Streptococcus mutans, Candida albicans, and Klebsiella sp.

The antimicrobial activity of SeNPs was evaluated using the agar well diffusion technique [Rifaath et al., 2023]. The wells were then filled with different concentrations (25, 50, 100 µg/mL) of SeNPs. An antibiotic (Amoxyrite, Flucanazole) was used as the standard. The plates were incubated at 37°C for 24 and 48 h for fungal cultures. The antibacterial efficacy was assessed by quantifying the diameter of the zone of inhibition (ZOI) encompassing the wells. The diameter of the ZOI was determined using a ruler and was thereafter documented in mm, after which the ZOI was estimated [Rifaath et al., 2023].

2.4 Time-kill curve analysis

A time-kill curve approach was used to evaluate the microbial characteristics of SeNPs, following previous research [Hameed et al., 2024]. The pathogens were cultivated in Mueller-Hinton broth supplemented with SeNPs, and their growth was quantified at regular intervals. To ensure the attainment of the mid-log phase by pathogens, preliminary growth curves were produced during a 5 h pre-incubation period in a broth devoid of antimicrobial agents. An inoculum with a size of 0.5 McFarland was, obtained from cultures cultured at 37° C for 18-20 h, was diluted in pre-warmed broth using pH-balanced saline (PBS). A 90 mL volume of the aforementioned combination was introduced into each well in a 96-well plate. Subsequently, 10 µL of SeNPs at several concentrations (25, 50, and 100 µg/mL) was added, and an untreated control was included for reference.

2.5 Protein leakage analysis

The isolation of microbial proteins into supernatants was used to evaluate the structural soundness of microbial cells. The microbiological suspensions consisting, of E. faecalis, S. mutans, C. albicans, and Klebsiella sp., were subjected to several concentrations of SeNPs (25, 50, and 100 µL), with each suspension containing 10 mL. Positive controls were established using microbial suspensions, whereas ampicillin and fluconazole were used as standard materials. Protein leakage analysis was conducted using a methodology akin to that outlined in previous studies.

2.6 Embryonic toxicology of SeNPs in zebrafish

The present study on embryonic toxicity in zebrafish was conducted a prior study [Rajeshkumar et al., 2022]. SeNPs synthesized using C. verum extract were administered to embryos at concentrations from 5-80 µg/mL. The study employed three replicates, and a control group, in the culture medium. The plates were subjected to incubation at 26°C, and various stages of embryo and larval development were periodically observed. The ratios of hatching and mortality were documented, whereas microscopic examination was conducted to observe malformations generated by nanoparticle interactions.

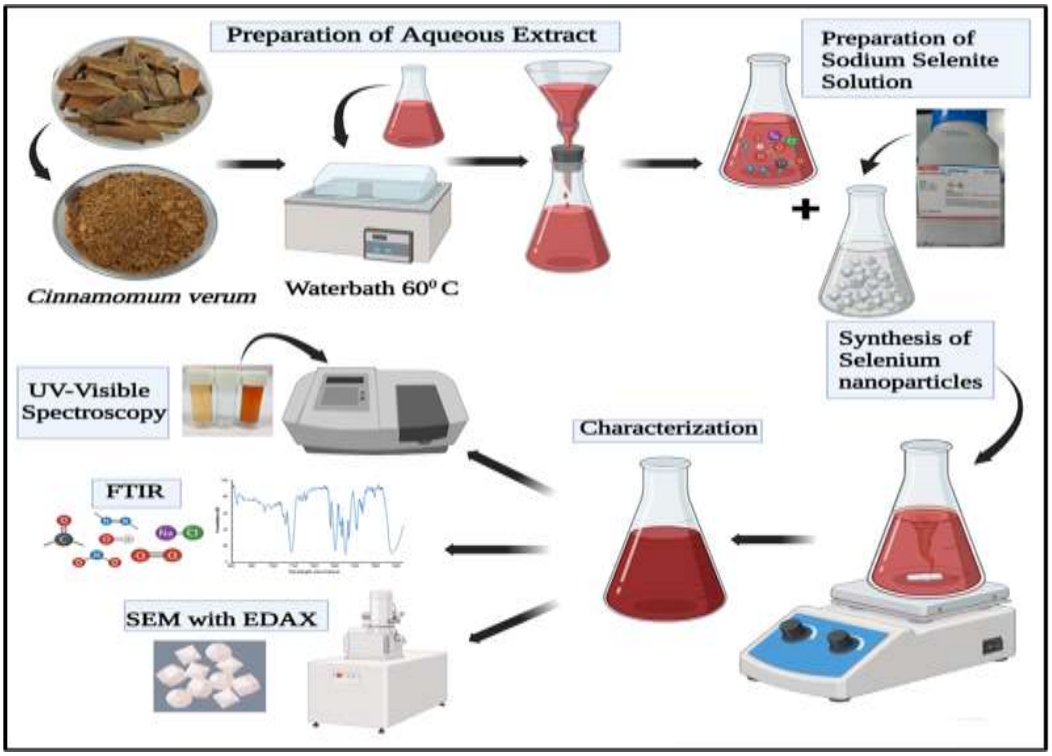

Figure 1: Graphical abstract of the synthesis of selenium nanoparticles by cinnamon extract.

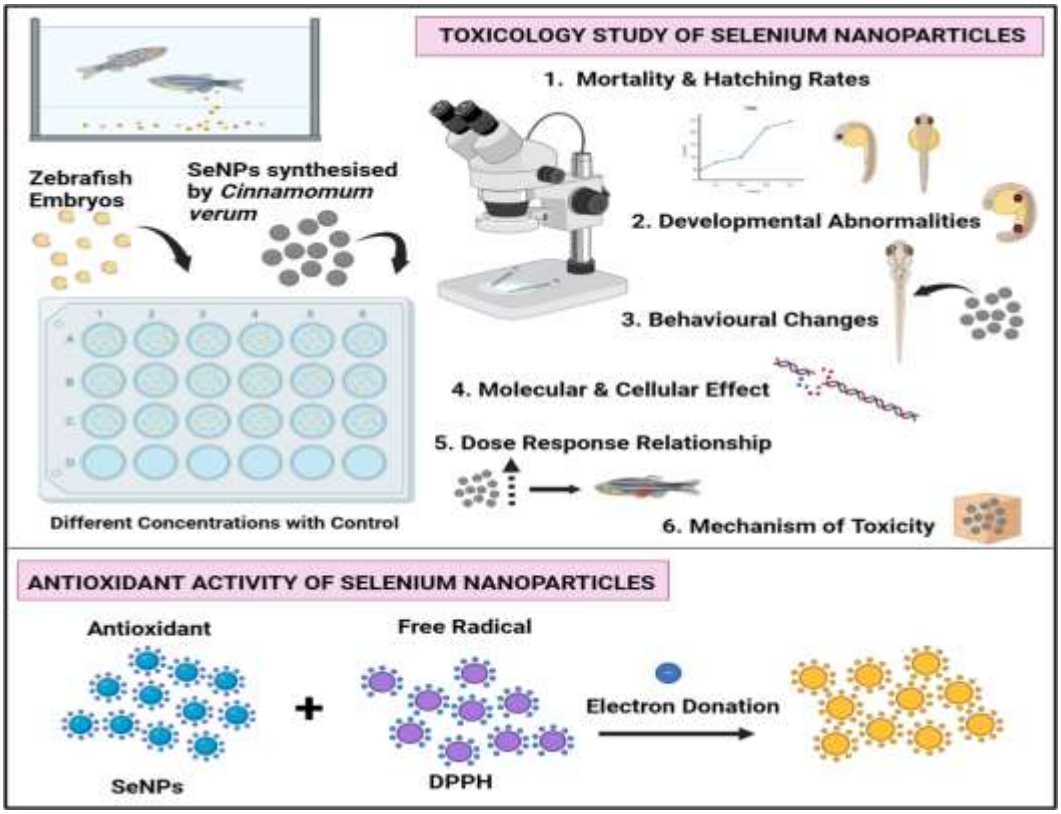

Figure 2: Graphical abstract of the toxicological study and antioxidant activity of the synthesized selenium nanoparticles

3. Results

3.1 UV-Visible Spectroscopy

To confirm the synthesis of SeNPs, UV/vis spectrophotometry in the range of 200-800 nm was performed and to examine the optical characteristics of green SeNPs synthesized from C. verum bark extract.

The UV-Vis absorbance spectrum shows a sharp peak around 210-230 nm and also indicates a red shift, as shown in Figure 3. This peak indicates a strong UV absorbance by the SeNPs in the corresponding wavelength range, which is typical for nanoparticles due to their unique electronic properties. The sharp peak at lower wavelengths (around 210-230 nm) can be attributed to electronic transitions within the SeNPs. These transitions are generally attributed to electron excitation from the valence band to the conduction band. The energy difference between these bands in the nanoparticles could result in typical absorbance bands in the UV region.

There is a noticeable secondary peak around 270-280 nm, although it is much smaller in intensity than the primary peak. This secondary peak suggests the presence of another electronic transition or the influence of the particle size and distribution on the absorbance properties of the SeNPs [Pyrzynska 2024]. The significant UV absorption of SeNPs demonstrates the product's suitability for various medicinal applications. The presence of a secondary peak and the overall shape of the absorbance spectrum can provide insights into the size distribution and surface characteristics of SeNPs. Smaller particles typically show a more pronounced absorbance in the UV region due to quantum confinement effects, where electronic properties are significantly altered due to the reduced dimensions of the NPs.

As the wavelength increases from 300 to 500 nm, the absorbance gradually decreases, approaching zero. The above observations reveal that the absorbance of SeNPs is higher in the UV region and is negatively inclined in the visible region. The lack of a distinct Surface Plasmon Resonance (SPR) peak in the visible region suggests that the SeNPs might be too small or not in the optimal size range for SPR in the visible spectrum [AL-Roomi and Ajeel 2024].

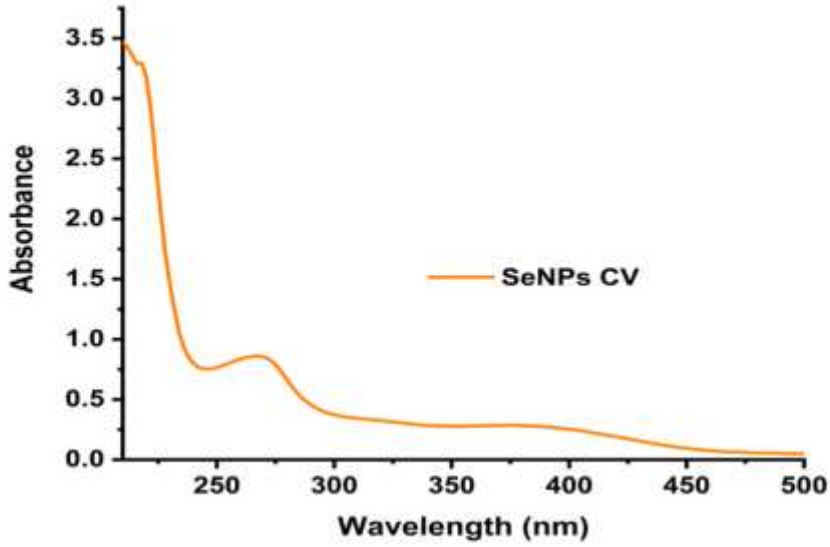

Figure 3: UV-Visible spectra of SeNPs from Cinnamomum extract

3.2 Fourier Transform Infrared Spectroscopy

To broaden the understanding of the roles of various functional groups between the reducing agent (Cinnamon extract) and Na_2SeO_3 in the formation of SeNPs, FTIR analysis was performed. All functional groups are represented as peaks in the FTIR spectra (**Figure 4)**. FTIR analysis was performed for samples in the range of 4000-400 cm-1. FTIR spectroscopy revealed prominent absorption bands at the peaks (3239.978, 1586.784, 1386.583,1189.809, 1096.331, 615.953, 487.535, 418.316 cm^{-1}).

The broad peak at 3239.978 cm^{-1} can be attributed to the O-H stretching of the hydroxyl groups. The presence of such groups indicates that water or alcohol is involved in the stabilization or capping of SeNPs. The bark extract likely contains water or alcohol, which contributes to this peak. 1586.583 cm^{-1} peak corresponds to the C=C stretching vibrations of the aromatic rings. This result is consistent with the presence of cinnamaldehyde, a major component of C. verum bark extract, which contains aromatic compounds. The peak at 1386.583 cm^{-1} is often associated with C-H bending vibrations in the methyl groups of organic compounds in the bark extract. The highest peak level is observed at 1189. 809 cm^{-1} is attributed to C-O stretching, a functional group normally observed in alcohols, ethers, carboxylic acids, or esters. This suggests that the bark extract contains such compounds that are interacting with the SeNPs. 1096.331 cm^{-1} band can be attributed to C-O-C stretching vibrations, indicating the presence of ether linkages or possibly the presence of secondary alcohols. The peak at 615.953 cm^{-1} indicates the presence of Se-O stretching vibrations, suggesting an interaction between Se and oxygen in the structure of the NPs. 487.535 cm^{-1} peak is due to the Se-Se stretching vibrations, indicating the formation of SeNPs. The peak at 418.316 cm^{-1} is also related to Se-O or Se-Se stretching vibrations, further supporting the formation of SeNPs.

The FTIR spectrum confirmed the successful synthesis of SeNPs, as indicated by the Se-O and Se-Se stretching vibrations. The presence of various organic functional groups such as hydroxyl, aromatic, and ether groups in the C. verum bark extract supports the positive contribution of these compounds to the reduction and stabilization of SeNPs [AL-Roomi and Ajeel 2024, Alghuthaymi et al., 2021].

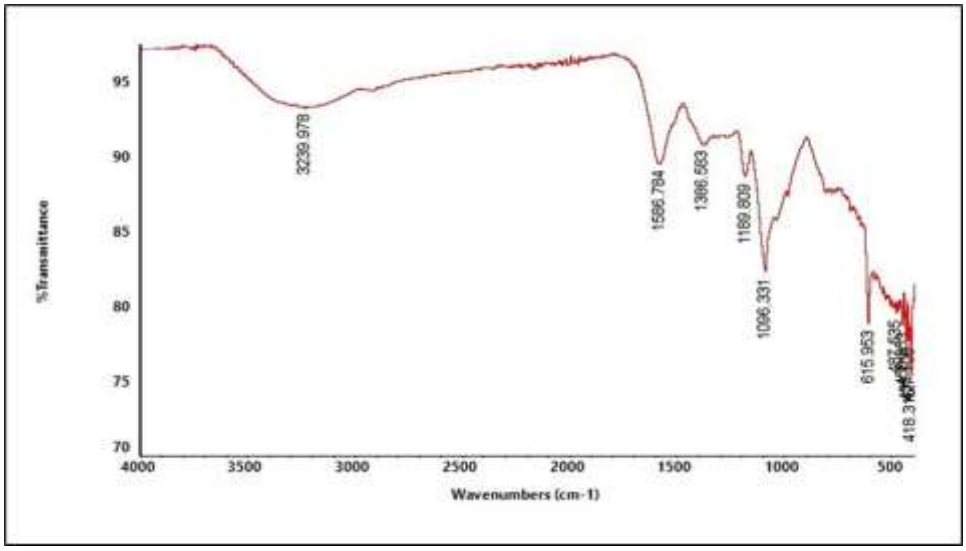

Figure 4: FTIR Spectra of SeNPs synthesized from Cinnamomum extract

3.3 SEM with EDAX

Figures 5 and 6 show the results of SEM analysis coupled with EDAX. The SEM image (Figure 5) reveals that the synthesized SeNPs are spherical, which is a common morphology of nanoparticles synthesized using biological methods. The shape uniformity suggests a consistent synthesis process. The nanoparticles appeared to be well-dispersed across the surface, indicating that the synthesis process effectively prevented significant agglomeration. This step is important for ensuring that the nanoparticles retain their unique properties and do not clump together. The scale bar at the bottom of the SEM image indicates a scale of 0.5 micrometers (µm). The average particle size was calculated as 50-100 nm. Based on these results, the SeNPs can be estimated to have a diameter in the range of tens of nanometers, typically expected for nanoparticles.

EDAX provides information on the qualitative and quantitative status of the elements concerned, which may be relevant in the formation of nanoparticles. The elemental analysis of the SeNPs synthesized from C. verum bark extract is illustrated in Figure 6. Key peaks in the spectrum correspond to different elements detected in the sample, including Carbon (C), Oxygen (O), Sodium (Na), Chlorine (Cl), Potassium (K), and Selenium (Se). Table 1 lists the morphological and surface characteristics of the SeNPs and the weight (Wt%) and atomic percentage of each element. The elemental profile is as follows: -

The high Carbon (48. 2 wt%), which can be attributed to the organic nature of the components in the C. verum bark extract used in the synthesis of the nanocomposite. These organic compounds, possibly including polyphenols and cinnamaldehyde, play major roles in the reduction and stabilization of SeNPs. The significant presence of Oxygen (41.6 wt%) is consistent with the presence of organic molecules that contain hydroxyl, carbonyl, and carboxyl groups. Additionally, oxygen might be associated with the SeNPs themselves if they are partially oxidized or if surface-adsorbed oxygen species are present. Potassium (4.2 wt%) was likely present in the C. verum bark extract, as potassium salts are commonly found in plant materials. It might also play a role in stabilizing nanoparticles. Sodium (3.1 wt%) could be present in any residual Na_2SeO_3 used as the selenium source in the synthesis. It indicates that not all sodium was removed during the purification process. Chlorine (1.6 wt%) may originate from any salts or compounds in the bark extract or the reaction medium. Its presence in a small amount suggests that it is a minor component. The presence of Selenium (1.4 wt%) confirmed the successful synthesis of SeNPs. Despite its lower percentage than other elements, its detection validates the formation of SeNPs [Behera et al., 2024b].

Together the SEM and EDX spectra provide a holistic view of the SeNPs. The SEM image confirmed the nanoscale size and spherical morphology of the particles, while the EDAX spectrum provided the elemental composition, confirming the successful synthesis and stabilization of SeNPs. The high carbon and oxygen contents determined from the EDAX analysis reinforce the idea that organic molecules from the bark extract are crucial to nanoparticle formation process [Keleşoğlu et al., 2023, Vyas and Rana 2017].

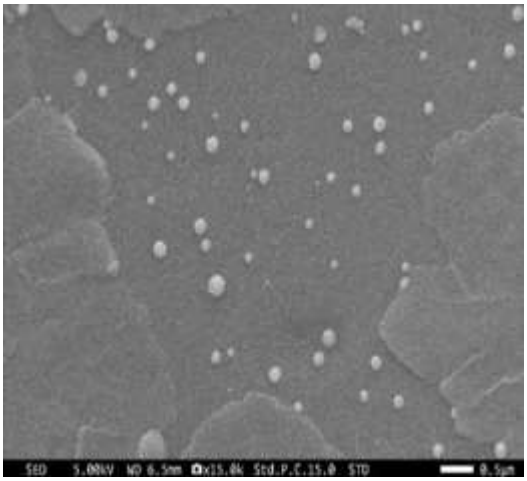

Figure 5: SEM images of SeNPs [Behera et al., 2024b]

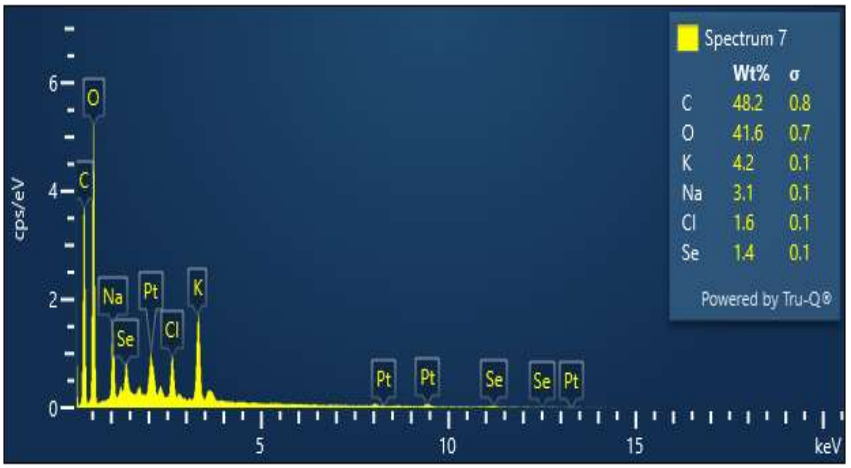

Figure 6: SEM EDAX images of SeNPs [Behera et al., 2024b]

Table 1. Elemental analysis of the SeNPs was performed using EDAX [Behera et al., 2024b]

S. No	Magnification	Average Particle Size (nm)	Morphology	Surface Characteristics	Element	Weight % (Wt%)	Atomic %
Sample 1	15.0 K	50-100	Spherical	Smooth	C	48.2	58.01
					O	41.6	37.55
					K	4.2	1.55
					Na	3.1	1.95
					Cl	1.6	0.65
					Se	1.4	0.26

3.4 Antioxidant Assay

3.4.1 DPPH Assay

The DPPH assay is widely used assay for determining the ability of compounds to scavenge free radicals. The percentage of DPPH radical scavenging activity was determined from the level of reduction in absorbance, which indicated the potency of the compound in consuming free radicals. Figure 7 shows the percentage inhibition of DPPH radicals by two samples: a standard antioxidant (depicted in red) and SeNPs (depicted in blue) at various concentrations ranging from 10 to 50 µg/mL.

Both standard and SeNPs showed an increase in the inhibition percentage with increasing concentration. The standard antioxidant consistently showed higher inhibition percentages compared with SeNPs at each concentration. It can be inferred that both the standard and SeNPs have significant antioxidant properties, as evidenced by their ability to inhibit DPPH radicals. The standard antioxidant showed superior efficacy compared with SeNPs at all tested concentrations. This suggests that although SeNPs have good antioxidant potential, they are not as potent as standard antioxidants. For both samples, the inhibition of DPPH radicals increased with increasing concentration, which is a typical antioxidant assay result. The increased inhibition suggests that higher concentrations of antioxidants are more effective at neutralizing free radicals, up to the highest tested concentration of 50 µg/mL. At 10 µg/mL, the standard exhibited approximately 64% inhibition, whereas the SeNPs exhibited approximately about 58% inhibition. This difference of approximately 6% means that the SeNPs are slightly less effective at lower concentrations. At a concentration of 50 µg/mL, the standard achieved an inhibition level of approximately 88%. The gap narrowed slightly at higher concentrations, suggesting that the difference in efficacy between the standard and SeNPs decreased as the concentration increased.

The higher efficacy of the standard antioxidant suggests that it may be more suitable for applications requiring strong and immediate antioxidative effects. SeNPs, although slightly less potent, still demonstrate substantial antioxidative activity, which could be advantageous in scenarios where natural or less potent antioxidants are preferred due to lower toxicity or better biocompatibility.

The DPPH assay data demonstrated that both the standard antioxidant and SeNPs had significant radical-scavenging abilities, with the standard showing consistently higher inhibition percentages. However, the substantial antioxidant activity of SeNPs highlights their potential as a natural antioxidant source. The increasing trend of inhibition with increasing concentration for both samples suggests a dose-dependent response, encouraging the exploration of higher concentrations or combinations with other antioxidants to enhance efficacy [Benitha et al., 2021].

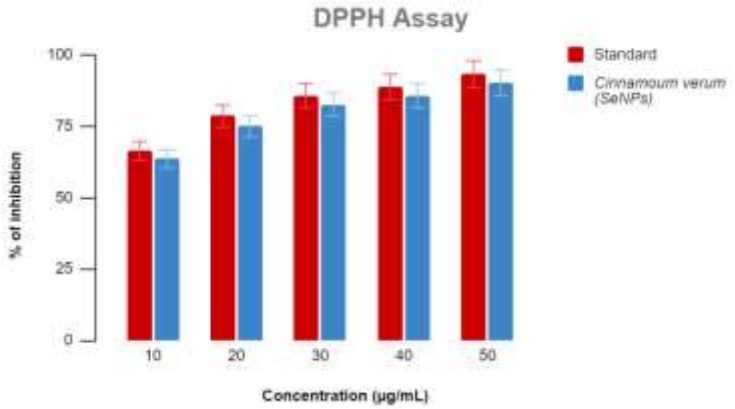

Figure 7: DDPH inhibition by SeNPs and Standard

3.4.2 Hydrogen Peroxide Scavenging Assay

SeNPs and the standard antioxidant showed a progressive increase in percent inhibition as the concentration range increases from 10µg/mL to 50µg/mL. This trend suggests a dose-dependent response, where higher concentrations result in greater inhibition of H_2O_2 production, indicating stronger antioxidant activity. The standard antioxidant shows approximately 50% inhibition, whereas SeNPs exhibit slightly lower inhibition, close to 45% at 10 µg/mL concentration. At 20 µg/mL concentration, the standard antioxidant inhibitory effect increased to approximately 55%, whereas SeNPs showed approximately 52% inhibition. The inhibition off the standard was approximately 65%, with SeNPs at approximately 60% when 30 µg/mL was used. At 40 µg/mL concentration, the standard antioxidant reaches approximately 75% inhibition, whereas the SeNPs exhibit approximately 70% inhibition. In the maximum concentration used (50 µg / mL), both the standard and SeNPs exhibited approximately 90% inhibitory effects, revealing highly potent antioxidant activity at this concentration.

Across all concentrations, SeNPs consistently showed slightly lower inhibition percentages than the standard antioxidant. However, the differences were not substantial, particularly at higher concentrations (40 and 50 µg/mL), where the percentage of inhibition converged. Results imply that SeNPs have potent antioxidant properties, although they are slightly less effective than standard antioxidants, particularly at lower concentrations. However, at higher concentrations, the effectiveness of SeNPs approached that of the standard, indicating that could be a viable alternative for antioxidant applications. The use of SeNPs derived from C. verum might enhance its antioxidant properties compared with non-nanoparticle forms, though further comparative studies are needed to confirm this.

The H_2O_2 assay results shown in Figure 8 indicate a clear dose-dependent inhibition of hydrogen peroxide by both the standard antioxidant and SeNPs. Although the standard antioxidant consistently showed slightly higher inhibition percentages, SeNPs also demonstrated significant antioxidant activity, particularly at higher concentrations. The small error bars suggest reliable and consistent data, reinforcing the potential of SeNPs as strong antioxidants, suitable for various applications in which oxidative stress must be mitigated [Shanmugam et al., 2023].

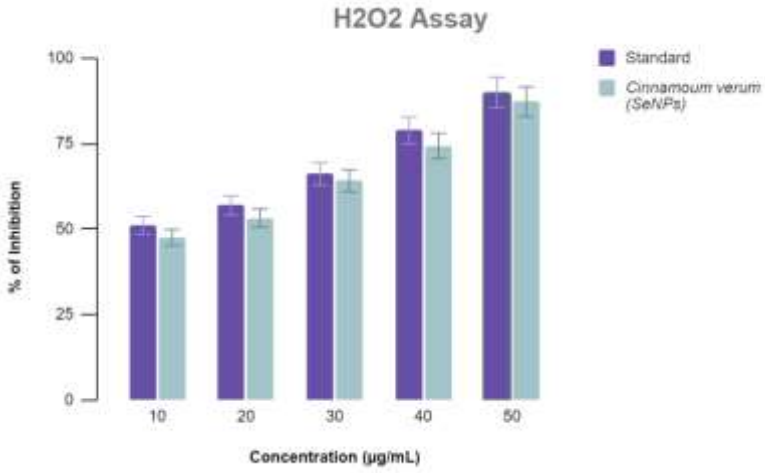

Figure 8: H_2O_2 inhibition of the SeNPs and Standard

3.4.3 FRAP Assay

One of the standard techniques for evaluating antioxidant activity is the FRAP method. This assay relies on the conversion of a relatively insoluble ferric-triazine complex to its less insoluble ferrous form, which can be detected by measuring the absorbance at 593 nm. The antioxidants present in the sample were in a position to reduce ferric (Fe^{3+}) to ferrous (Fe^{2+})

ions, thereby increasing the absorbance. This variation in absorbance is directly related to the antioxidant activity of the sample.

Absorbance readings obtained from the spectrophotometer indicated the antioxidant capacity of the samples. Increased absorbance correlates with higher antioxidant potential as ferric ions are reduced to ferrous ions by the antioxidants in the extracts. At low concentrations (10 µg/mL), the absorbance was relatively low. This suggests that the amount of antioxidants present in the sample was minimal; hence, the reduction of ferric ions and the percentage of inhibition is limited. At moderate concentrations (20, 30 µg/mL), as the extract concentration increases, a corresponding increase in absorbance is observed. This indicates that higher levels of antioxidants are available to reduce ferric ions. At high concentrations (40, 50 µg/mL), the absorbance was significantly higher than at lower concentrations. This suggests the substantial presence of antioxidants, leading to a greater reduction in ferric ions. The highest concentration (50 µg/mL) exhibited the maximum absorbance and percentage of inhibition, indicating a peak antioxidant activity within the tested range.

Both the standard and SeNPs exhibit antioxidant activity, and the activity increases with increasing concentration. The SeNPs extract shows slightly lower antioxidant activity than the standard at all tested concentrations, which is clearly illustrated in **Figure 9** [Vyas and Rana 2017].

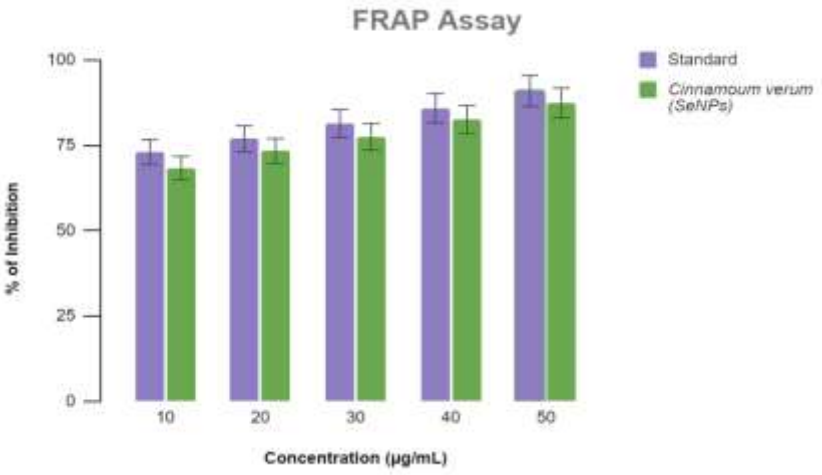

Figure 9: FRAP inhibition by SeNPs and Standard

3.4.4 ABTS Assay

Figure 10 shows the results of an ABTS assay comparing, the antioxidant activities of a standard substance and SeNPs at different concentrations (50, 40, 30, 20, and 10µg/mL). The y-axis represents the percentage of inhibition, indicating the extent to which the SeNPs can neutralize the ABTS radical, which is a common method for measuring antioxidant activity.

The results revealed that both the standard and SeNPs exhibited antioxidant activities, as indicated by their ability to inhibit ABTS radicals at all concentrations. The percentage of inhibition increased with increasing concentration for both substances, suggesting a dose-dependent relationship.

At low concentrations (10 µg/mL), the standard exhibited slightly higher inhibition (68%) compared with SeNPs (65%). This trend continued at 20 µg/mL (standard 73%, SeNPs 70%) and 30 µg/mL (standard 76%, SeNPs 73%). At higher concentrations (40 and 50 µg/mL), the differences in anti-oxidant activity between the standard and the SeNPs diminish. Both treatments reached approximately the same level of inhibition (79% at 40 µg/mL and 82% at 50 µg/mL).

SeNPs are highly effective antioxidants, performing nearly and the standard at all tested concentrations. This effect is particularly notable at higher concentrations where the difference in effectiveness between the standard and the nanoparticles is minimal. The high percentage of inhibition achieved by SeNPs suggests that these nanoparticles could be a potent source of antioxidant activity, potentially due to their surface properties or increased reactivity owing to their nanoscale size.

The close performance of SeNPs to the standard antioxidant suggests that these nanoparticles can be used as an alternative to conventional antioxidants in various applications, such as food preservation, cosmetics, and health supplements. The ability of SeNPs to effectively scavenge free radicals at relatively low concentrations also highlights their potential utility in reducing oxidative stress in biological systems, which is linked to various diseases, including ageing and cancer [Vyas and Rana 2017].

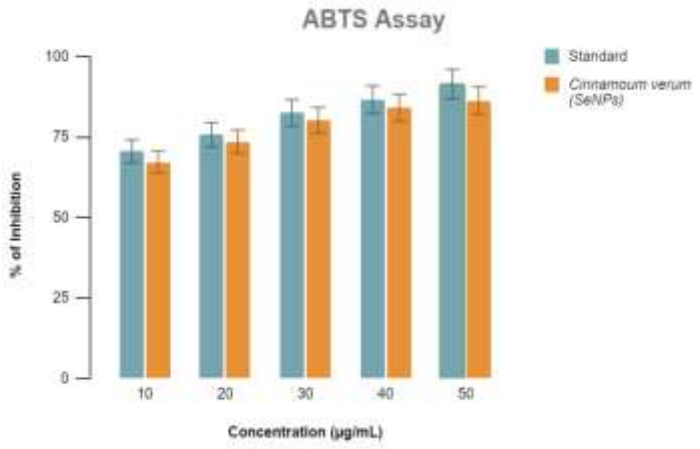

Figure 10: ABTS inhibition by SeNPs and Standard

3.4.5 Nitric Oxide Scavenging Assay

Both standard and SeNPs showed a dose-dependent increase in nitric oxide inhibition as their concentrations increased. As shown in Figure 11, At all tested concentrations, the standard exhibited slightly higher inhibition percentages compared to SeNPs. This suggests that the standard substance is marginally more effective at inhibiting nitric oxide production. For both substances, the percentage of inhibition increased with increasing concentration. This indicates a positive dose-response relationship, which is typical in pharmacological assays. The incremental increases in inhibition appear to be consistent, suggesting a stable and predictable response to increasing concentrations.

Although SeNPs as nitric oxide inhibitors are not as potent as the standard, they significantly inhibit nitric oxide. This could have potential therapeutic implications, especially in conditions where nitric oxide plays a role, such as inflammation and cardiovascular diseases. The data indicate that SeNPs can be developed as a natural, plant-based therapeutic agent with applications under certain conditions [Abedi et al., 2021].

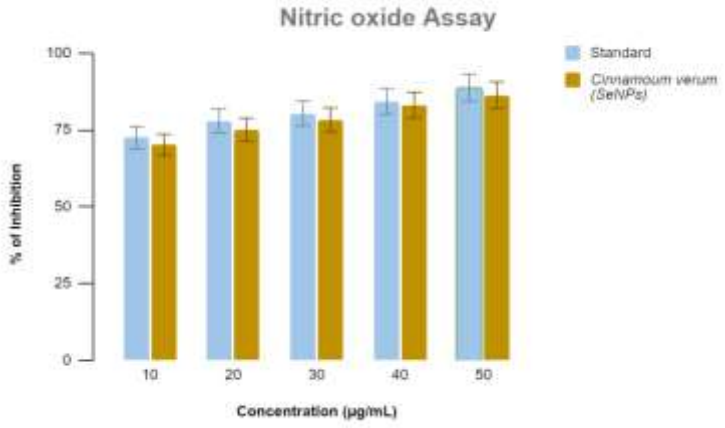

Figure 11: Nitric oxide inhibition by SeNPs and Standard

3.5 Antimicrobial Activity

As shown in Figure 12, the ZOI of SeNPs was demonstrated against three different bacteria (Klebsiella sp., Streptococcus mutans, Enterococcus faecalis) and one fungal culture (Candida albicans). Figure 13 illustrates the antimicrobial activity of SeNPs synthesized from C. verum extract. The activity was measured against Enterococcus faecalis, Streptococcus mutans, Klebsiella sp., and Candida albicans using the agar well diffusion method, where the ZOI (measured in mm) indicates the effectiveness of the antimicrobial agent.

SeNPs synthesized from C. verum extract exhibit antimicrobial activity against all tested microorganisms. There was a dose-dependent increase in the ZOI for all microorganisms, indicating that higher SeNPs concentrations resulted in greater antimicrobial activity. The

control, which likely represents a standard antimicrobial agent, exhibited a significantly higher ZOI (~30 mm) compared with the SeNPs at all tested concentrations.

The SeNPs were less effective than the control but still demonstrated measurable antimicrobial properties. All four microorganisms exhibited similar sensitivities to SeNPs, as indicated by the relatively consistent ZOI across the tested concentrations. This suggests that SeNPs have broad-spectrum antimicrobial activity against, both Gram-negative bacteria (Klebsiella sp.), Gram-positive bacteria (S. mutans and E. faecalis) and fungi (C. albicans). This confirms the dose-response relationship, which shows an increase in the ZOI as the concentration of SeNPs increases. At 25 µg/mL, the ZOI are around 7-8 mm, increasing slightly to 8-9 mm at 50 µg/mL, and reaching 9-10 mm at 100 µg/mL.

The present data suggest that SeNPs synthesized from C. verum extract could serve as alternative or complementary antimicrobial agents, particularly in cases where traditional antibiotics are ineffective or resistance is an issue. The ability of SeNPs to inhibit various microorganisms highlights their potential use in treating various infections, including those caused by bacteria and fungi [Benitha et al., 2021].

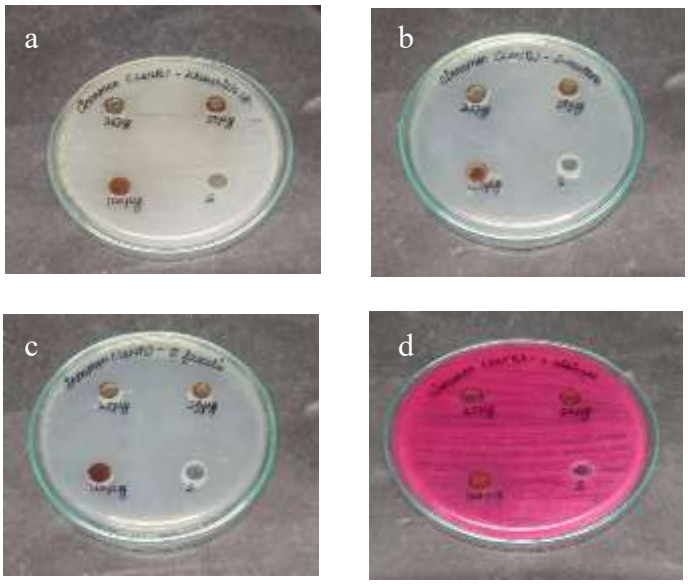

Figure 12: ZOI of SeNPs against (a) Klebsiella sp., (b) S. mutans, (c) E. faecalis, (d) C. albicans

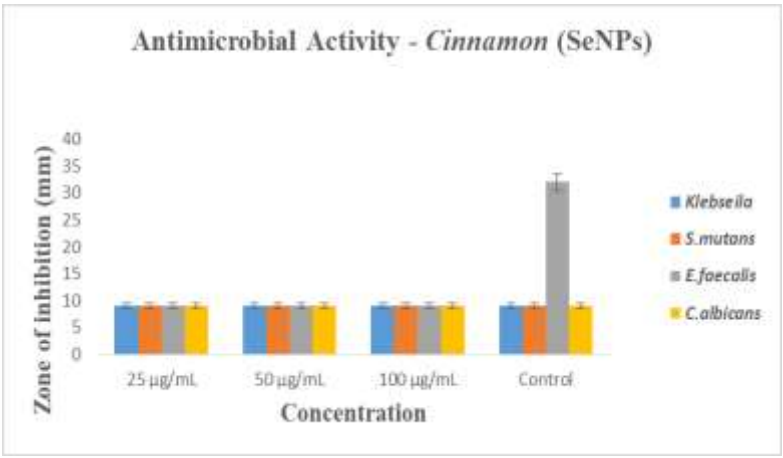

Figure 13: Antimicrobial activities of SeNPs

3.6 Time-Kill Kinetic Analysis

Figure 14 displays the results of a time-kill curve analysis conducted to assess the bactericidal properties of SeNPs formulated with C. verum extract against four different pathogens: Klebsiella sp., S. mutans, E. faecalis, and C. albicans. Each panel represents a different microorganism and shows the bacterial load (in Log CFU/mL) over time (0 to 5 h), treated with different concentrations of SeNPs (25 µg/mL, 50 µg/mL, 100 µg/mL), standard antibiotic treatment, and untreated control.

Across all pathogens, the curves show little to no reduction in bacterial load over the 5 h period for all tested SeNPs concentrations. The consistency of the curves, including the controls, indicated that SeNPs at the tested concentrations did, not significantly reduce the bacterial load. The "standard" treatment line in each graph remained closely aligned with the SeNPs treatments and the control, indicating similar ineffectiveness in reducing the pathogen populations. This may suggest a potential resistance to the standard treatment or general tolerance of the pathogens to the treatments under the tested conditions. The responses of each pathogen to the treatments is remarkably similar, which could indicate that the mode of action of SeNPs and the standard treatment may not be sufficiently potent or fast-acting against these particular strains.

In conclusion, the time-kill curve analysis presented in the graphs demonstrates a critical examination point for the ongoing development of nanoparticle-based antimicrobial treatments. The apparent lack of significant antimicrobial activity at the tested concentrations and conditions highlights the complexity of developing effective nanoparticle-mediated therapies against robust pathogens [dos Santos Souza et al., 2022].

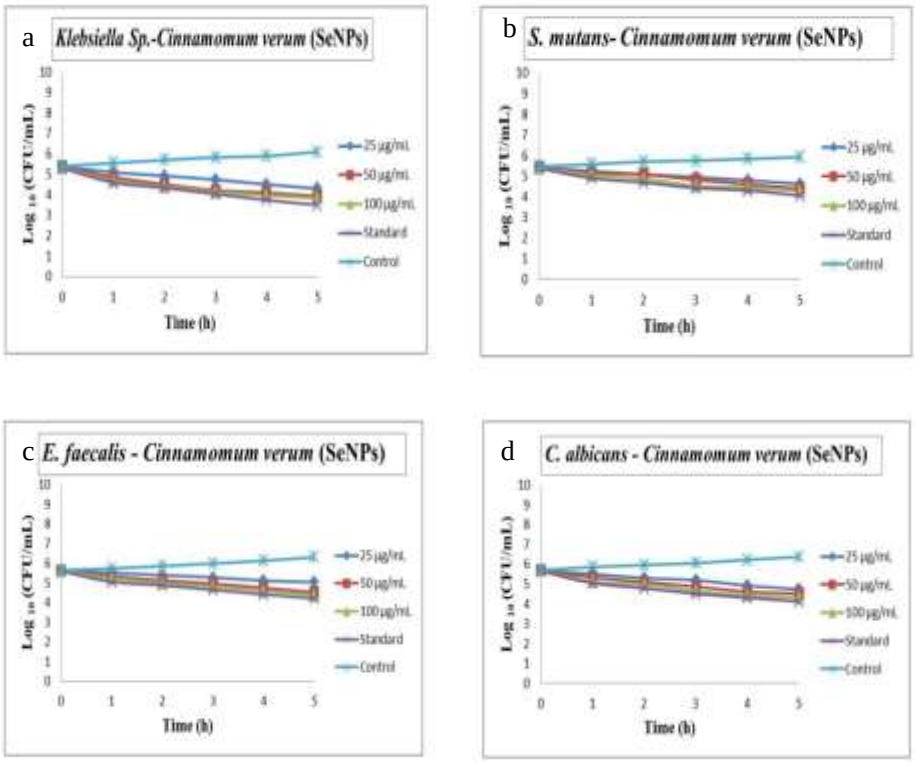

Figure 14: Time kill curve analysis of SeNPs

3.7 Protein Leakage Analysis

Figure 15 presents protein leakage analysis of various microorganisms (E. faecalis, S. mutans, Klebsiella sp., and C. albicans) treated with cinnamon-derived SeNPs at different concentrations. This study aims to assess the antimicrobial properties of these nanoparticles, specifically their ability to induce protein leakage, which is a marker of cellular damage.

Across all organisms, as the concentration of SeNPs increased from 25 µg/mL to 100 µg/mL, the optical density tended to remain relatively stable, suggesting that increasing the SeNPs concentration within this range does not significantly enhance protein leakage. This could indicate a threshold above which higher concentrations do not increase cellular damage or, that the method of action of the plateaus of these nanoparticles is within this range.

E. faecalis and S. mutans exhibited similar optical density patterns across concentrations, suggesting similar sensitivity or resistance to SeNPs-induced stress. Klebsiella sp. showed a similar trend but generally had slightly higher optical density values at each concentration,

possibly indicating a higher degree of susceptibility to SeNPs or greater protein leakage. As a fungal organism, C. albicans generally exhibits a pattern similar to that of bacterial strains, but with lower optical density values. This suggests that C. albicans is either less affected by SeNPs or has different mechanisms of resistance or response to these nanoparticles.

The standard likely refers to a treatment considered effective for inducing protein leakage and, used as a benchmark to evaluate the efficacy of SeNPs. The optical densities for the standard treatment across the microbial strains were consistent and aligned closely with those observed for high concentrations of SeNPs, suggesting that SeNPs at 100 µg/mL perform similarly to the standard treatment. The control group, which had the lowest optical density, served as the baseline, indicating the level of protein leakage in the absence of any treatment. Significantly lower values confirm the role of SeNPs in inducing protein leakage.

It can be suggested that cinnamon-derived SeNPs induce protein leakage across various microbial strains at the tested concentrations, with no significant gain observed at higher concentrations within the tested range. The behavior across different strains indicates that although there is a general effectiveness of the nanoparticles, the degree and pattern of responses may vary slightly among different types of microorganisms. This type of analysis is crucial for determining the potential of SeNPs as antimicrobial agents, especially for determining effective concentrations and predicting broad-spectrum capabilities [Elakraa et al., 2022].

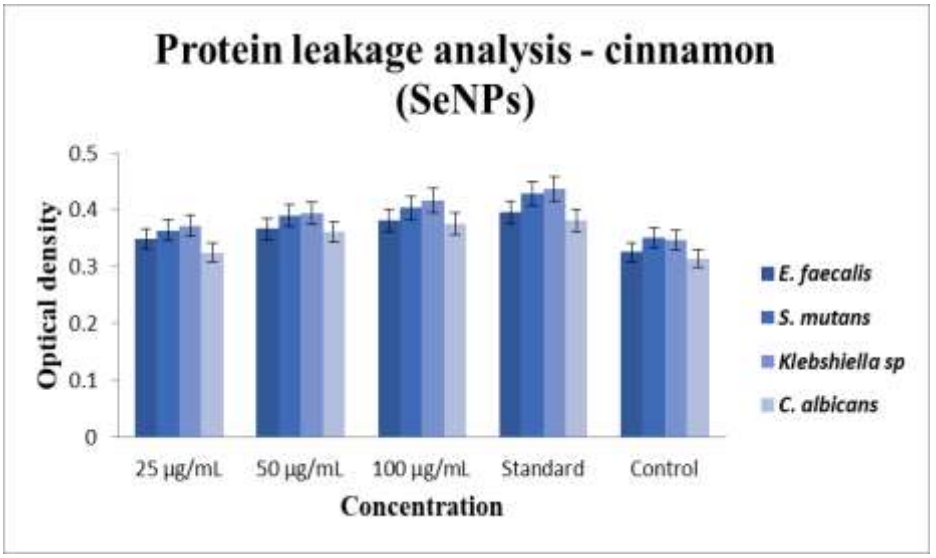

Figure 15: Protein leakage analysis of microorganisms

3.8 Toxicology of Selenium Nanoparticles in Zebrafish Embryos

Zebrafish embryos have been established as an in vivo assay model and can be used as a preclinical model for drug development for human diseases. Zebrafish and human organisms share 85% genome similarity. To analyze the cytotoxicity of SeNPs, zebrafish embryos were treated with SeNPs at concentrations of 5–80 μg/mL.

Figure 16 shows zebrafish embryos at different stages of development exposed, to various concentrations of SeNPs: (a) 4 h, (b) 24 h, and (c) 48 h. The first image depicts a normal embryo, whereas the other two images show signs of malformation or developmental abnormalities, indicating the toxic effects of SeNPs.

Figure 16: Microscopic images of Selenium nanoparticles in zebrafish embryo recorded at different periods (a) 4 h, (b) 24 h, and (c) 48 h.

3.8.1 Different stages of Zebrafish embryo development

Figure 17 depicts the results of toxicity assays performed on Zebrafish embryos exposed to various concentrations of SeNPs. The first graph shows the hatching rate of the embryos. As the concentration of NPs increased, the hatching rate decreased, indicating that SeNPs hinder the hatching process. The second graph illustrates the viability rate of zebrafish embryos. Similar to the hatching rate, the viability rate decreased with increasing SeNPs concentration, suggesting that SeNPs are toxic to zebrafish embryos and reduce their survival. Overall, the data indicate that SeNPs have a toxic effect on zebrafish embryos, causing developmental abnormalities and reducing hatching and viability rates [Pérez Gutiérrez et al., 2022].

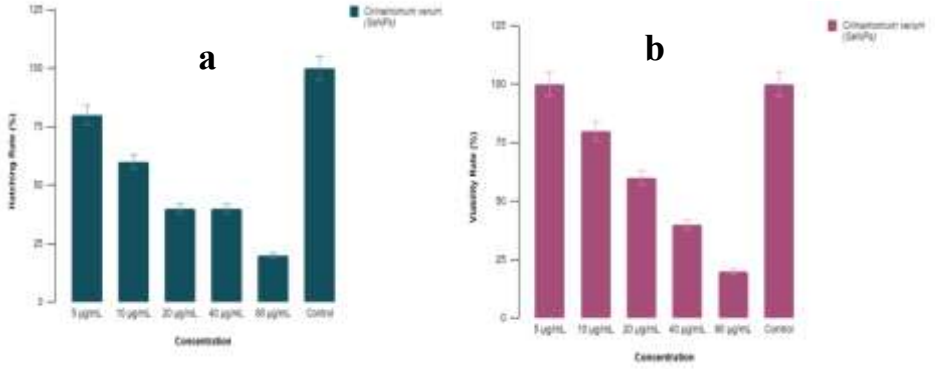

Figure 17: Toxicity analysis of SeNPs on Zebrafish embryos (a) Hatching rate and (b) Viability rate

4. Discussion

The bioreduction of SeNPs was further supported by characteristic analytical techniques focusing on the successful use of C. verum bark extract in the synthesis of SeNPs. UV-Visible spectroscopy analysis revealed a CIE peak at 210-230 nm and the second at 270-280 nm due to electronic transitions of the nanoparticles. These peaks indicate that the material exhibits excellent UV absorption and that it is possible to be affected by the size and distribution of SeNPs [Pyrzynska 2024, AL-Roomi and Ajeel 2024]. In FTIR spectroscopy, the absorption bands indicated some wavenumbers present in the functional groups of C. verum bark extract that were responsible for the reduction and stabilization of SeNPs. Notably, the peaks attributed to Se-O and Se-Se vibrations served as confirmation that SeNPs were synthesized; however, the role of the extract was evident from the signals of the hydroxyl, aromatic, and ether groups [Alghuthaymi et al., 2021]. The features of SeNPs were characterized by SEM and EDAX analyses, which revealed information related to the morphology and elemental assessment. The high percentage values of carbon and oxygen in the encapsulated NPs were attributed to the significant contribution of organic compounds in the bark extract to the stabilization of NPs [Keleşoğlu et al., 2023].

The antioxidant activity of SeNPs was determined using various methods. The result obtained from the DPPH assay was also significant radical scavenging activity with inhibition increasing with the concentration of SeNPs. SeNPs were found to come close to the standard antioxidant but possessed less antioxidant activity as compared to it; however, at increased concentrations, SeNPs demonstrated appreciable antioxidant activity [Benitha et al., 2021]. The same results were obtained in the H_2O_2 scavenging assay, in which the antioxidant activity increased with increasing SeNPs concentration and was close to the standards at higher concentrations [Shanmugam et al., 2023]. The antioxidant activity of SeNPs was also established to be significant in both the FRAP and ABTS assays; however, the ABTS assay provided a better estimation of the strong antioxidant properties of the nanoparticles. SeNPs

also exerted a great extent of inhibition in the nitric oxide scavenging assay, which indicates their therapeutic relevance in diseases mediated by nitric oxide. Susceptibility of Klebsiella sp. to other microorganisms and their antifungal properties. Thus, they established that SeNPs possessed significant antimicrobial characteristics against several microorganisms, including both gram-positive and gram-negative bacteria, including Streptococcus mutans, Enterococcus faecalis, and Candida albicans [Vyas and Rana 2017]. SeNPs were, however, less effective than the control, but the ZOI increased with the increases in doses, which points to the fact that SeNPs can possibly be used as an alternative or adjunct to the currently available antimicrobial agents [Abedi et al., 2021, dos Santos Souza et al., 2022]. A time-kill kinetic analysis, however, showed moderate activity of SeNPs in preventing the growth of microorganisms at established concentrations; therefore, the current concentrations of SeNPs need to be optimized if better antimicrobial members are to be recorded [Elakraa et al., 2022].

This study demonstrated the successful green synthesis of SeNPs using the extract of C. verum bark and demonstrated the effective antioxidant and antimicrobial potential of the synthesized SeNPs. Thus, the approach of synthesizing nanoparticles using natural plant extracts not only addresses environmental concerns but also increases the biocompatibility of nanoparticles for their numerous applications in the biomedical field. Another direction for research should be devoted to improving the synthesis process and expanding the applications of such nanoparticles for various purposes in medicine and industry.

5. Conclusion:

The green synthesis of SeNps using an aqueous extract of cinnamon was confirmed by structural and morphological investigation. The existence of SeNPs was indicated by the absorbance peak observed at approximately 220 nm. Similarly, SeNPs were detected using FTIR and SEM with EDAX, leading to the identification of functional groups and the observation of a spherical particle shape. These findings indicate that this material may exhibit reduced environmental toxicity. The current study also involved the evaluation of antibacterial and antioxidant properties, and toxicological consequences, of SeNPs in zebrafish. Furthermore, it is important to conduct a more extensive and comprehensive clinical inquiry to evaluate the effects of this intervention on cancer treatment.

Declaration of interest

The authors declare that they have no known competing financial interests or personal relationships that could have appeared to influence the work reported in this paper.

Funding

This research did not receive any specific grant from any funding agency in the public, commercial or not-for-profit sector.

Author contribution statement

AB: Conceptualization, Data curation, Formal analysis, Investigation, Methodology, Validation, Visualization, Writing - original draft, and Writing - review & editing. **GP:** Conceptualization, Data curation, Formal analysis; Investigation, Methodology, Validation,

Visualization, Writing - original draft, and Writing - review & editing. **VS:** Conceptualization, Data curation, Formal analysis; Investigation, Methodology, Validation, Visualization, Writing - original draft, and Writing - review & editing. **IR:** Conceptualization, Data curation, Formal analysis; Investigation, Methodology, Validation, Visualization, Writing - original draft, and Writing - review & editing. **MKDJ:** Conceptualization, Data curation, Formal analysis; Investigation, Methodology, Validation, Visualization, Writing - original draft, and Writing - review & editing.

References

Abedi, S., Iranbakhsh, A., Oraghi Ardebili, Z., & Ebadi, M. (2021): Nitric oxide and selenium nanoparticles confer changes in growth, metabolism, antioxidant machinery, gene expression, and flowering in chicory (Cichorium intybus L.): potential benefits and risk assessment. Environ. Sci. Pollut. Res, 28, 3136-3148. https://doi.org/10.1007/s11356-020-10706-2

Abu-Elghait M, Hasanin M, Hashem AH, Salem SS. (2021): Ecofriendly novel synthesis of tertiary composite based on cellulose and myco-synthesized selenium nanoparticles: Characterization, antibiofilm and biocompatibility. Int J Biol Macromol. 175:294-303. https://doi.org/10.1016/j.ijbiomac.2021.02.040

Alagesan V, Venugopal S. (2019): Green synthesis of selenium nanoparticles using leaves extract of withania somnifera and its biological applications and photocatalytic activities. BioNanoScience. 9: 105-16. https://doi.org/10.1007/s12668-018-0566-8

Alghuthaymi MA, Diab AM, Elzahy AF, Mazrou KE, Tayel AA, Moussa SH. (2021): Green biosynthesized selenium nanoparticles by cinnamon extract and their antimicrobial activity and application as edible coatings with nano-chitosan. Journal of Food Quality. 2021:1-0. https://doi.org/10.1155/2021/6670709

AL-Roomi, N. M., & Ajeel, H. H. (2024): Antibacterial Effect of Green Synthesis of Selenium Nanoparticles against Salmonella typhi in Small Buffalo. Uttar Pradesh Journal of Zoology, 45(5), 80-90. https://doi.org/10.56557/upjoz/2024/v45i53933

Ansari MA, Murali M, Prasad D, Alzohairy MA, Almatroudi A, Alomary MN, Udayashankar AC, Singh SB, Asiri SM, Ashwini BS, Gowtham HG. (2020): Cinnamomum verum bark extract mediated green synthesis of ZnO nanoparticles and their antibacterial potentiality. Biomolecules. 10(2):336. https://doi.org/10.3390/biom10020336

Behera A, Jothinathan MK, Saravanan S, Selvan ST, Renuka RR, Srinivasan GP. (2024a): Green synthesis of selenium nanoparticles from clove and their toxicity effect and anti-angiogenic, antibacterial and antioxidant potential. Cureus. Mar;16(3). https://doi.org/10.7759/cureus.55605

Behera Archana, Devi M.S Yamuna, Ryntathiang Iadalin, Dharmalingam Jothinathan Mukesh Kumar, (2024b): Green Synthesis of Selenium Nanoparticles Using Cinnamomum verum Extract and Their Antibacterial, Antioxidant, and Brine Shrimp Toxicity Effects. Texila International Journal of Public Health. TJ2322. (in press). Texila International e-Journal (texilajournal.com)

Benitha, J., Ramani, P., Rajeshkumar, S., Gheena, S., Abhilasha, R., & Reshma, K. (2021): Antibacterial and Antioxidant Activity of Garcinia mangostana Mediated Selenium

Induced Nanoparticles: An In vitro Study. J. Pharm. Res. Int, 33(62A), 490-500. http://dx.doi.org/10.9734/jpri/2021/v33i62A35672

Bi SB, Elahi I, Sardar N, Ghaffar O, Ali H, Alsubki RA, Iqbal MS, Attia KO, Abushady AM. (2024): Exploring Non-Cytotoxic, Antioxidant, and Anti-Inflammatory Properties of Selenium Nanoparticles Synthesized from Gymnema sylvestre and Cinnamon cassia Extracts for Herbal Nanomedicine. Microb. Pathog. 106670. https://doi.org/10.1016/j.micpath.2024.106670

Chandramohan S, Sundar K, Muthukumaran A. (2019): Hollow selenium nanoparticles from potato extract and investigation of its biological properties and developmental toxicity in zebrafish embryos. IET nanobiotechnol. 13(3):275-81. https://doi.org/10.1049/iet-nbt.2018.5228

dos Santos Souza, L. M., Dibo, M., Sarmiento, J. J. P., Seabra, A. B., Medeiros, L. P., Lourenço, I. M., ... & Nakazato, G. (2022): Biosynthesis of selenium nanoparticles using combinations of plant extracts and their antibacterial activity. Curr. Res. Green Sustain. 5, 100303. https://doi.org/10.1016/j.crgsc.2022.100303

Elakraa, A. A., Salem, S. S., El-Sayyad, G. S., & Attia, M. S. (2022): Cefotaxime incorporated bimetallic silver-selenium nanoparticles: promising antimicrobial synergism, antibiofilm activity, and bacterial membrane leakage reaction mechanism. RSC Adv, 12(41), 26603-26619. https://doi.org/10.1039/d2ra04717a

Ghaderi RS, Adibian F, Sabouri Z, Davoodi J, Kazemi M, Amel Jamehdar S, Meshkat Z, Soleimanpour S, Daroudi M. (2022): Green synthesis of selenium nanoparticle by Abelmoschus esculentus extract and assessment of its antibacterial activity. Mater Technol. 37(10):1289-97. https://doi.org/10.1080/10667857.2021.1935602

Gulcin I, Kaya R, Goren AC, Akincioglu H, Topal M, Bingol Z, Cetin Çakmak K, Ozturk Sarikaya SB, Durmaz L, Alwasel S. (2019): Anticholinergic, antidiabetic and antioxidant activities of cinnamon (Cinnamomum verum) bark extracts: polyphenol contents analysis by LC-MS/MS. Int. J. Food Prop. 22(1):1511-26. https://doi.org/10.1080/10942912.2019.1656232

Gulcin İ. (2020): Antioxidants and antioxidant methods: An updated overview. Arch. Toxicol. 94(3):651-715. https://doi.org/10.1007/s00204-020-02689-3

Hameed S, Antony SD, Shanmugam R. (2024): Assessing the Antimicrobial Efficacy of Triple Antibiotic Paste (Tap) and Nano Silica-Enhanced Tap (Tap-N) against Enterococcus Faecalis: A Time Kill Curve Assay Study. Afr. J. Bio. Sc. 6(11), 1516-1524. https://doi.org/10.33472/AFJBS.6.11.2024.1516-1524

Haque E, Ward AC. (2018): Zebrafish as a model to evaluate nanoparticle toxicity. Nanomaterials. 8(7):561. https://doi.org/10.3390/nano8070561

Hariharan S, Chauhan S, Marcharla E, Alphonse CR, Rajaretinam RK, Ganesan S. (2024): Developmental toxicity and neurobehavioral effects of sodium selenite and selenium nanoparticles on zebrafish embryos. Aquat. Toxicol. 266: 106791. https://doi.org/10.1016/j.aquatox.2023.106791

Keleşoğlu, G. S., Özdinçer, M., Dalmaz, A., Zenkin, K., & Durmuş, S. (2023): Green synthesis and structural characterization of ZnO nanoparticle and ZnO@ TiO2 nanocomposite by Cinnamomum verum bark extract. TurkJAC. 5(2), 118-123. https://doi.org/10.51435/turkjac.1395817

Munteanu IG, Apetrei C. (2021): Analytical methods used in determining antioxidant activity: A review. Int J Mol Sci. 22(7): 3380. https://doi.org/10.3390/ijms22073380

Pérez Gutiérrez, R. M., Soto Contreras, J. G., Martínez Jerónimo, F. F., de la Luz Corea Téllez, M., & Borja-Urby, R. (2022): Assessing the ameliorative effect of selenium Cinnamomum verum, Origanum majorana, and Origanum vulgare nanoparticles in diabetic zebrafish (Danio rerio). Plants, 11(7), 893. https://doi.org/10.3390/plants11070893

Pyrzynska, K. (2024): Plant Extracts for Production of Functionalized Selenium Nanoparticles. Materials, 17(15), 3748. https://doi.org/10.3390/ma17153748

Rajakumari R, Volova T, Oluwafemi OS, Rajesh Kumar S, Thomas S, Kalarikkal N. (2020): Grape seed extract-soluplus dispersion and its antioxidant activity. Drug development and industrial pharmacy. 46(8):1219-29. https://doi.org/10.1080/03639045.2020.1788059

Rajeshkumar S, Santhoshkumar J, Vanaja M, Sivaperumal P, Ponnanikajamideen M, Ali D, Arunachalam K. (2022): Evaluation of zebrafish toxicology and biomedical potential of aeromonas hydrophila mediated copper sulfide nanoparticles. Oxid. Med. Cell. Longev. 2022(1):7969825. https://doi.org/10.1155/2022/7969825

Rifaath M, Rajeshkumar S, Anandan J, Munuswamy T, Govindharaj S, Shanmugam R, Jayasree A, Munusamy T, Sulochana G. (2023): Preparation of herbal nano-formulation-assisted mouth paint using titanium dioxide nanoparticles and its biomedical applications. Cureus. 15(11). https://doi.org/10.7759/cureus.48332

Salem SS, Badawy MS, Al-Askar AA, Arishi AA, Elkady FM, Hashem AH. (2022): Green biosynthesis of selenium nanoparticles using orange peel waste: Characterization, antibacterial and antibiofilm activities against multidrug-resistant bacteria. Life. 12(6): 893. https://doi.org/10.3390/life12060893

Shanmugam, R., Anandan, J., Balasubramanian, A. K., Raja, R. D., Ranjeet, S., & Deenadayalan, P. (2023): Green synthesis of selenium, zinc oxide, and strontium nanoparticles and their antioxidant activity-a comparative in vitro study. Cureus, 15(12). https://doi.org/10.7759/cureus.50861

Vinothkanna A, Mathivanan K, Ananth S, Ma Y, Sekar S. (2023): Biosynthesis of copper oxide nanoparticles using Rubia cordifolia bark extract: characterization, antibacterial, antioxidant, larvicidal and photocatalytic activities. Environ. Sci. Pollut. Res. 30(15):42563-74. https://doi.org/10.1007/s11356-022-18996-4

Vyas, J., & Rana, S. H. A. F. K. A. T. (2017): Antioxidant activity and biogenic synthesis of selenium nanoparticles using the leaf extract of Aloe vera. Int. J. Curr. Pharm. Res, 9, 147-152. http://dx.doi.org/10.22159/ijcpr.2017v9i4.20981

Wu S, Rajeshkumar S, Madasamy M, Mahendran V. (2020): Green synthesis of copper nanoparticles using Cissus vitiginea and its antioxidant and antibacterial activity against urinary tract infection pathogens. Artif Cells Nanomed Biotechnol. 48(1):1153-8. https://doi.org/10.1080/21691401.2020.1817053

Yilmaz MT, İspirli H, Taylan O, Dertli E. (2021): A green nano-biosynthesis of selenium nanoparticles with Tarragon extract: Structural, thermal, and antimicrobial characterization. Lwt. 141: 110969. https://doi.org/10.1016/j.lwt.2021.110969